RICHTMYER-MESHKOV INSTABILITIES IN STRATIFIED FLUIDS

Karnig O. Mikaelian

Based on a talk given at the 25th Annual Meeting of the APS Division of Plasma Physics, November 7-11, 1983, Los Angeles, California

December 16, 1983

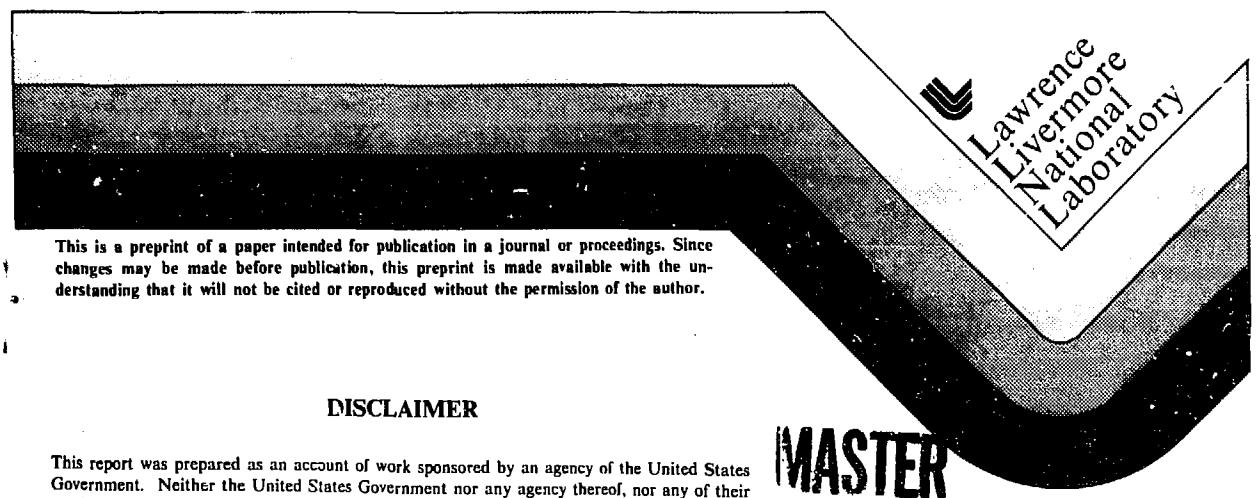

RICHTMYER-MESHKOV INSTABILITIES IN STRATIFIED FLUIDS*

Karnig O. Mikaelian

Lawrence Livermore National Laboratory

University of California

Livermore, California 94550

Abstract

We present an analytic theory of Richtmyer-Meshkov instabilities in an arbitrary number N of stratified fluids subjected to a shock. Following our earlier work on Rayleigh-Taylor instabilities, the theory assumes incompressible flow in which a shock is treated as an impulsive acceleration, $g = \Delta v\, \delta(\tau - \tau_s)$, Δv being the jump velocity induced in the system by a shock at time τ_s. We discuss the special cases N = 2 and N = 3, and illustrate both Rayleigh-Taylor and Richtmyer-Meshkov instabilities by examples patterned after Inertial Confinement Fusion implosions.

*Work performed under the auspices of the U.S. Department of Energy by the Lawrence Livermore National Laboratory under Contract No. W-7405-ENG-48.

I. INTRODUCTION

The Rayleigh-Taylor[1,2] instability occurs in systems undergoing a constant acceleration, while the Richtmyer-Meshkov[3,4] instability occurs in systems which have been impulsively accelerated by a shock. For both types of instabilities the classical case is a system of two semi-infinite fluids of densities ρ_1 and ρ_2, with perturbations of wavelength λ at their common interface. If the acceleration is constant (R-T case) then these perturbations grow exponentially in time,

$$\eta/\eta(o) = e^{\gamma\tau} \quad , \quad \gamma = \sqrt{gkA} \qquad \text{(R-T case)} \tag{1}$$

where g is the acceleration directed from ρ_1 to ρ_2, $k = 2\pi/\lambda$, and $A = (\rho_2 - \rho_1)/(\rho_2 + \rho_1)$ is the Attwood number. If the acceleration is impulsive (R-M case) then the perturbations grow linearly in time,

$$\eta/\eta(o) = 1 + \gamma\tau \quad , \quad \gamma = \Delta v k A \qquad \text{(R-M case)} \tag{2}$$

where Δv is the jump velocity caused by the passage of a shock from ρ_1 to ρ_2. In Eqs. (1) and (2) η is the amplitude of the sinusoidal perturbations and τ stands for time.

Equation (2), derived by Richtmyer,[3] is based on the same assumptions that go into the derivation of the classical Rayleigh-Taylor result, Eq. (1). Both equations are valid only in the small amplitude, or linear, regime. The fluids are assumed to be incompressible with no viscosity or surface tension, and heat transfer is neglected. Detailed numerical calculations by Richtmyer[3] showed good agreement with Eq. (2) if the instantaneous reduction in amplitude due to shock compression was taken into account. Experiments by Meshkov[4] confirmed the prediction that amplitudes grow linearly with time after the passage of a shock. As the amplitude grows the linear approximation

and hence Eq. (2) are no longer valid: turbulent mixing takes place. Subsequent experiments[5] observed this mixing and a semi-empirical model was developed.

Recently we generalized[6] the results of the classical R-T instability to a system of an arbitrary number N of stratified fluids (see Fig. 1). In this paper we derive the corresponding equations for the R-M instability. The classical results, Eqs. (1) and (2), will be special cases given by N = 2.

We would like to point out that our work is still based on the six simplifying assumptions (linearity, incompressibility, etc.) that go into the derivation of the classical Eqs. (1) and (2). Our theory only extends the simple classical density profile of two fluids with one interface to an arbitrary density profile of N fluids with N - 1 interfaces. In actual applications, for example in Inertially Confined Fusion (ICF) targets where density gradients arise naturally, these six assumptions must be kept in mind.

The plan of the paper is as follows: in Section II we derive the general equation describing how perturbations evolve in time after the passage of a shock. In Section III we consider the special cases N = 2 and N = 3. In Section IV we make several numerical applications involving various combinations of shocks and constant accelerations patterned after ICF implosions. Finally, a number of comments and conclusions are given in Section V.

II. DERIVATION OF THE GENERAL EQUATION

Figure 1 shows the system and some of our notation: N fluid layers of densities $\rho_1, \rho_2, \ldots, \rho_N$ and thicknesses $t_1, t_2, \ldots, t_N$.

There are N - 1 interfaces and η_i is the amplitude of perturbations (of wavelength λ) at the interface between ρ_i and ρ_{i+1}.

We showed in Ref. 6 that there are N - 1 eigenvalues γ_ℓ and associated eigenfunctions W^ℓ obtained by solving

$$MW = \frac{gk}{\gamma^2} W \tag{3}$$

where M is a (N - 1) x (N - 1) tri-diagonal dimensionless matrix, the elements of which depend only on kt_i and the ratios ρ_i/ρ_{i+1}. Expanding in terms of these eigenfunctions we derived[7] a general equation which describes how the amplitude η_i at interface i evolves in time:

$$\eta_i(\tau) = \sum_{\ell=1}^{N-1} \sum_{j=1}^{N-1} W(i,\ell)\, W^{-1}(\ell,j) \{\eta_j(o) \cosh(\gamma_\ell \tau) + [\dot{\eta}_j(o)/\gamma_\ell] \sinh(\gamma_\ell \tau)\} \tag{4}$$

(for more details see Refs. 6 and 7). We have assumed so far that the acceleration g is constant, so that Eq. (4) is the generalization of Eq. (1) for the R-T case.

To obtain the corresponding equation for the R-M case, we use a technique similar to the one used by Richtmyer[3] in obtaining Eq. (2). From Eq. (4),

$$\frac{d^2\eta_i(\tau)}{d\tau^2} = g \sum_{\ell=1}^{N-1} \sum_{j=1}^{N-1} \Gamma_\ell^2\, W(i,\ell)\, W^{-1}(\ell,j) \{\eta_j(o) \cosh(\gamma_\ell \tau) + [\dot{\eta}_j(o)/\gamma_\ell] \sinh(\gamma_\ell \tau)\} \tag{5}$$

where we have defined $\gamma_\ell^2 = g\Gamma_\ell^2$. With this definition, Γ_ℓ is independant of g since γ_ℓ^2 is proportional to g (see Eq. (3)).

Following Ref. 3 we represent a shock by an impulsive acceleration, i.e., let $g = \Delta v\, \delta(\tau - \tau_s)$, where τ_s is the shock arrival time. This implies that $g = 0$ immediately before ($\tau < \tau_s$) and immediately after ($\tau > \tau_s$) the shock. Actually we can treat the case where the shock is immediately preceded and/or followed by a finite acceleration (see Section IV) but in this Section we treat the case of an isolated shock for clarity.

Substituting $g = \Delta v\, \delta(\tau - \tau_s)$ in Eq. (5) and integrating twice, we get

$$\eta_i(\tau) = \eta_i(o) + \dot{\eta}_i(o)\tau + \Delta v \sum_{\ell=1}^{N-1} \sum_{j=1}^{N-1} \Gamma_\ell^2\, W(i,\ell) W^{-1}(\ell,j)\, x$$

$$\{\eta_j(o) + \dot{\eta}_j(o)\tau_s\}\, \{\tau - \tau_s\}\, \theta(\tau - \tau_s) \quad . \qquad (6)$$

This is the equation which generalizes Eq. (2) for the case of the R - M instability.

Before considering special cases and applications of Eq. (6) we note a few points. As in Eq. (4) we see that all the modes, indicated by the summation over ℓ, contribute to the time evolution of $\eta_i(\tau)$ at each interface $i = 1, 2, \ldots, N - 1$. Similarly, the initial conditions at all the interfaces, indicated by the summation over j, contribute to $\eta_i(\tau)$. Note that since $\eta_j(o) + \dot{\eta}_j(o)\tau_s = \eta_j(\tau_s)$, it is actually the instantaneous values of η_j at shock time τ_s that influence $\eta_i(\tau)$ (of course, this instantaneous value is related to the initial conditions).

As seen from Eq. (6), the effect of the shock is to change the rate of change $d\eta_i/d\tau$: the amplitude η_i itself is not immediately affected by the shock: $\eta_i(\tau_{s+}) = \eta_i(\tau_{s-})$ where $\tau_{s\pm}$ refer to times immediately before and

after the shock. The amplitude remains the same but its slope is changed suddenly so that $\dot{\eta}_i(\tau_{s+}) \neq \dot{\eta}_i(\tau_{s-})$. As discussed in the above paragraph, this change depends on the instantaneous values of the amplitudes at all the interfaces including the one in question (the sum over j includes j = i).

We now consider special cases of Eq. (6) which illustrate the above remarks and also have interesting properties.

III. SPECIAL CASES

A. N = 2

This is the classical case considered by Richtmyer.[3] The density profile is shown in Fig. 2a. Since there is only one interface and only one term in the sum indicated in Eq. (6), we drop the subscripts. Of course $\Gamma^2 = \gamma^2_{classical}/g = kA = k(\rho_2 - \rho_1)/(\rho_2 + \rho_1)$, and we get

$$\eta(\tau) = \eta(o) + \dot{\eta}(o)\tau + \Delta v\, k\left(\frac{\rho_2 - \rho_1}{\rho_2 + \rho_1}\right)\{\eta(o) + \dot{\eta}(o)\tau_s\}\{\tau - \tau_s\}\,\theta(\tau - \tau_s) \qquad (7)$$

We are considering a system of two semi-infinite fluids moving under the action of an isolated shock: between $\tau = o$ and $\tau = \tau_s$ the system is coasting at some constant velocity v(o). At $\tau = \tau_s$ a shock induces a jump velocity Δv and after $\tau = \tau_s$ the system coasts with velocity $v(o) + \Delta v$. The jump occurs instantaneously at $\tau = \tau_s$. Perturbations at the interface, which may have been increasing/decreasing linearly with time until $\tau = \tau_s$, continue to evolve linearly in time but with a new slope given by $\dot{\eta}(o) + \Delta v k A \eta(\tau_s)$. If the initial conditions read $\dot{\eta}(o) = \tau_s = 0$, then

$$\eta(\tau)/\eta(o) = 1 + \Delta v k A \tau \qquad \text{(R-M case)} \qquad (8)$$

which agrees with the result derived in Ref. 3.

It is clear from Eq. (8) that, following a shock, perturbation amplitudes can increase or decrease depending on the sign of ΔvA. If the shock proceeds from low to high density ($\Delta vA > 0$) then perturbations increase, while a shock proceeding from high to low density ($\Delta vA < 0$) causes perturbations to decrease. However, if the system continues to coast, perturbations in the second case simply go through zero, i.e., change phase, and continue to grow in absolute magnitude.

For the Rayleigh-Taylor case of constant acceleration g, Eq. (8) is replaced by

$$\eta(\tau)/\eta(o) = \cosh(\sqrt{kgA}\,\tau) \qquad \text{(R-T case)} \tag{9}$$

again assuming $\dot{\eta}(o) = 0$. For $gA < 0$, i.e., high density fluid accelerating low density fluid, the system is stable and $\eta(\tau)$ oscillates in time and never grows any larger than its initial value as long as the system continues to accelerate in the same direction. We conclude that while the distinction between stable and unstable cases $gA < 0$ and $gA > 0$ is clear for R-T instabilities, that distinction becomes somewhat blurred for R-M instabilities where perturbations grow in magnitude for both cases $\Delta vA > 0$ and $\Delta vA < 0$.

We now take advantage of Eq. (7), which is general and accommodates arbitrary initial conditions, to analyze all possible cases of how $\eta(\tau)$ can evolve after the passage of a shock at $\tau = \tau_s$. There are 15 possibilities, not all of which are allowed for a given sign of ΔvA. These are shown in Fig. 3. For a "stable" shock, i.e., $\Delta vA < 0$, Fig. 3a - 3i are allowed while the rest are not allowed. For an "unstable" shock, i.e., $\Delta vA > 0$, only Figs. 3i - 3o are allowed. The two simplest cases with $\dot{\eta}(o) = 0$ are shown in Fig. 3a and Fig. 3j; the rest are obtained by

considering a positive or negative $\dot{\eta}(o)$ and short or long shock arrival time τ_s. One may imagine, for example, that the initial conditions were set by a first shock at $\tau = 0$ and the perturbations evolve until a second shock arrives at $\tau = \tau_s$. The effect of this second shock is to change $\dot{\eta}$ by an amount equal to $\Delta vkA\eta(\tau_s)$.

We will discuss only a few out of the 15 cases shown in Fig. 3. Figure 3i is the case $\eta(\tau_s) = 0$ in which case neither a "stable" shock nor an "unstable" shock has any effect on the perturbation. Of course, this happens if the second shock is timed to arrive exactly at $\tau_s = -\eta(o)/\dot{\eta}(o)$.

Perhaps the more interesting cases are shown in Figs. 3c, 3g and 3n, where the amplitude is "frozen out" and remains constant after the shock. Obviously this is achieved when the slope change caused by the second shock exactly cancels the slope set by the previous one. Timing must be such that the interval time between the two shocks is

$$\tau_s^* = -\frac{\dot{\eta}(o) + \Delta vkA\eta(o)}{\Delta vkA\dot{\eta}(o)} \quad . \tag{10}$$

It is interesting to point out that this "freezing out" of the amplitude can be achieved with a "stable" shock ($\Delta vA < 0$) in both cases of $\dot{\eta}(o) > 0$ or $\dot{\eta}(o) < 0$, as indicated in Figs. 3c and 3g, while an "unstable" shock ($\Delta vA > 0$) can freeze out an amplitude only if it previously was decreasing, i.e., $\dot{\eta}(o) < 0$, as indicated in Fig. 3n.

Finally, we point out that it is, unfortunately, impossible to "freeze out" an amplitude as it passes through zero.

B. N = 3

The system consists of three fluid layers of densities ρ_1, ρ_2 and ρ_3, with $t_1 = t_3 = \infty$. The eigenvalues and eigenfunctions for

arbitrary densities were given previously[6,7] and will not be repeated here. Instead, we will consider the more specialized case of $\rho_1 = \rho_3 = 0$, i.e., a single fluid with two free boundaries as shown in Fig. 2b. This system was treated by Taylor[2] for the case of a constant acceleration.

As indicated in Fig. 2b, we let ρ and t denote the density and thickness respectively of the "middle" layer ($\rho_2 = \rho$ and $t_2 = t$). The results are independent of ρ since the eigenvalue equation, Eq. (3), involves only the ratios of densities. Furthermore, t appears only in the combination kt.

The two eigenvalues are $\Gamma_1^2 = -\Gamma_2^2 = k$, and the eigenfunctions are $W(1, 1) = W(2, 2) = 1$, $W(1, 2) = W(2, 1) = e^{-kt}$. The elements of the inverse matrix W^{-1} are

$$W^{-1}(1, 1) = W^{-1}(2, 2) = \frac{1}{1 - e^{-2kt}} \quad ,$$

$$W^{-1}(1, 2) = W^{-1}(2, 1) = -\frac{e^{-kt}}{1 - e^{-2kt}} \quad . \tag{11}$$

Substituting these expressions in Eq. (6) we obtain

$$\eta_1(\tau) = \eta_1(o) + \dot{\eta}_1(o)\tau + \frac{\Delta v k}{1-e^{-2kt}} \left\{(1 + e^{-2kt})\,(\eta_1(o) + \dot{\eta}_1(o)\tau_s) - 2e^{-kt}(\eta_2(o) + \dot{\eta}_2(o)\tau_s)\right\}(\tau - \tau_s)\,\theta(\tau - \tau_s) \quad , \tag{12}$$

$$\eta_2(\tau) = \eta_2(o) + \dot{\eta}_2(o)\tau - \frac{\Delta v k}{1-e^{-2kt}} \left\{(1 + e^{-2kt})(\eta_2(o) + \dot{\eta}_2(o)\tau_s) - 2e^{-kt}(\eta_1(o) + \dot{\eta}_1(o)\tau_s)\right\}(\tau - \tau_s)\,\theta(\tau - \tau_s) \quad . \tag{13}$$

Clearly, $\eta_2(\tau) = \eta_1(\tau)$ with $1 \leftrightarrow 2$ and $\Delta v \rightarrow -\Delta v$. Our convention is that a positive Δv indicates a shock directed from ρ_1 to ρ_2.

At short wavelengths λ or, equivalently, at large thicknesses t, i.e., $kt >> 1$, the two interfaces decouple and the two Eqs. (12) and (13) each reduce to Eq. (7) with an Attwood number of ± 1. In the opposite limit of long wavelength or small thickness t, i.e. $kt << 1$, the two interfaces "see" each other and the evolution at one interface depends very much on the other.

Let us consider the case $\dot{\eta}_1(o) = \dot{\eta}_2(o) = \eta_2(o) = \tau_s = 0$. The system is shown in Fig. 4: initially only one of the free surfaces is perturbed with amplitude η_o, while the other surface is perfectly smooth. Then,

$$\frac{\eta_{perturbed}}{\eta_o} = 1 + \frac{\Delta v k}{1-e^{-2kt}} (1 + e^{-2kt})\tau \quad , \tag{14}$$

$$\frac{\eta_{smooth}}{\eta_o} = 2 \frac{\Delta v k e^{-kt}}{1-e^{-2kt}} \tau \quad . \tag{15}$$

The corresponding equations for the case of R-T instability, i.e., g = constant, are

$$\frac{\eta_{perturbed}}{\eta_o} = \frac{1}{1-e^{-2kt}} \left\{ \cosh(\sqrt{gk}\,\tau) - e^{-2kt} \cos(\sqrt{gk}\,\tau) \right\} \quad , \tag{16}$$

$$\frac{\eta_{smooth}}{\eta_o} = \frac{e^{-kt}}{1-e^{-2kt}} \left\{ \cosh(\sqrt{gk}\,\tau) - \cos(\sqrt{gk}\,\tau) \right\} \quad . \tag{17}$$

Eqs. (14)-(17) illustrate how an initial perturbation at one interface can induce perturbations at the other interface. The convention in Eqs. (14)-(17) is that a positive Δv or g indicates a shock or a constant acceleration directed from the perturbed surface towards the smooth surface.

In this case perturbations at both surfaces grow with the same phase as the initial amplitude η_0.

For a shock or a constant acceleration in the opposite direction, i.e., from a smooth surface towards a perturbed surface, Δv or g is negative. Equations (14)-(17) show that in this case perturbations at the initially smooth surface develop in phase opposite to η_0 while the perturbations at the other surface decrease, go through zero, and eventually grow in phase opposite to their original amplitude η_0. In the case of R-M instability, the decrease is linear in time, while in the case of R-T instability, the amplitude may oscillate a few times (depending on the value of kt) before it grows large with a phase opposite to η_0.

It is clear that even in this simple case of a single fluid with two free surfaces the perturbations at each surface can evolve in a rather complicated manner. This is particularly true if the system is subjected to a series of shocks or accelerations in different directions. We illustrate with a number of numerical applications in the next Section.

IV. APPLICATIONS

In this Section we illustrate the numerical application of our technique with the case N = 5. We have written a code that can handle an arbitrary number of fluid layers undergoing an arbitrary velocity history, and a brief description of it will be useful.

The input to the code consists of the following four items: (i) the density profile, which is specified as densities $(\rho_1, \rho_2, \ldots, \rho_N)$ and thicknesses $(t_1, t_2, \ldots, t_N)$; (ii) the wavelength λ. Using the ratios ρ_i/ρ_j and t_i/λ the code calculates N - 1 eigenvalues γ_ℓ

and their associated eigenfunctions W(i, ℓ), and then inverts the matrix W. Next we need (iii) the velocity history of the system, which must consist of either constant or impulsive accelerations - this will tell the code to use Eq. (4) or Eq. (6) to evolve the perturbations in time. Finally, we need (iv) the initial conditions $\eta_i(o)$ and $\dot{\eta}_i(o)$, the initial amplitude and its initial rate of change at each interface i.

The output of the code consists of $\eta_i(\tau)$, the amplitude of the perturbation at each interface i at time τ. We also keep track of the distance covered by the system.

We now turn to a specific example with N = 5. The densities are (0, 1, 2, 4, 0) and the thicknesses are (∞, t/3, t/3, t/3, ∞). This density profile is shown in Fig. 2c. It was chosen for two reasons: first, it is representative of the density profile in ICF capsules where a shell of thickness t is driven from one side by low density plasma and compresses low density fuel on the other side. With this picture in mind, we will call the first interface, between ρ = 0 and ρ = 1, the "outer surface" of the shell, and the last interface, between ρ = 4 and ρ = 0, will be called the "inner surface". The reader must keep in mind that the geometr assumed in all our calculations is planar (see Fig. 1) and not spherical as suggested by the terms "inner" and "outer".

The second reason for choosing this admittedly simple density profile is that we can obtain analytic expressions for its four eigenvalues. Two of the eigenvalues are given by γ^2/gk = + 1 and - 1, and the other two are

$$\frac{\gamma^2}{gk} = \frac{S(1 + ST)(R^2 - 1) \pm S|R - 1| \sqrt{R}}{R^2 + R + 1 + S^2(R + 1)^2} \tag{18}$$

where $S = \sinh(kt/3)$ and $T = \tanh(kt/6)$, and R is the common ratio of densities $R = \rho_4/\rho_3 = \rho_3/\rho_2$ which is equal to 2 for the density profile shown in Fig. 2c. We used these equations as a check of our numerical calculation.

We have not specified the units for the densities since an overall scale is immaterial: the density profile (0, 1, 2, 4, 0) is equivalent, for example, to (0, 3, 6, 12, 0).

For our next input, the wavelength, we chose $\lambda = 3t$. Several considerations led to this choice: as expected, very long ($\lambda >> t$) wavelength perturbations grow too slowly, while very short ($\lambda << t$) wavelength perturbations grow very fast. For reasonable assumptions on surface finish, as discussed below, the very short wavelength perturbations grow so large that they are well outside the linear regime where our theory is applicable. Furthermore, the time evolution of very short wavelength perturbations is given to a good degree of accuracy by the classical expressions, Eqs. (1) and (2), applied at each interface independently. The interaction among the various interfaces, which is the main feature of our approach, becomes dominant at relatively longer wavelengths.

For our initial conditions, we chose the initial perturbations to be stationary, i.e., $\dot{\eta}_1(o) = \dot{\eta}_2(o) = \dot{\eta}_3(o) = \dot{\eta}_4(o) = 0$. As to the amplitudes themselves, we chose $\eta_2(o) = \eta_3(o) = 0$ and $\eta_1(o) \equiv \eta_{outside}(o) = \eta_4(o) \equiv \eta_{inside}(o) = \eta(o)$, that is we chose to start with no perturbation within the fluids and with equally rough initial surface finish $\eta(o)$ on the "inside" and "outside" surfaces. As the surface perturbations η_1 and η_4 evolve in time the fluid develops internal

perturbations, i.e. η_2 and η_3 grow from their initial zero value to rather large values as they are driven by the surface perturbations.

As another possible set of initial conditions we chose all $\eta_i(0) = 0$ except $\eta_4(0)$, corresponding to a shell whose outer surface is polished perfectly smooth and which starts with perturbations only on the inside. We found that this did not necessarily suppress the late time growth of the perturbations.

The final input, the velocity history, consisted of five different cases shown as diagram (a) in Figs. 5 to 9. These velocity histories illustrate possible ICF capsule implosions though, as mentioned earlier, the geometry assumed in Eqs. (4) and (6) is planar.

All our velocity histories are combinations of shocks and constant accelerations. In all cases we assumed that a final shock at $\tau = 5$ brings the shell to rest ($v = 0$), though of course in a capsule the shell would slow down, turn around and move out. Our velocity histories represent fuel burn at about $\tau \simeq 5$, though we will continue to evolve our equations up to $\tau = 6$ to show the effect of a large shock which proceeds from "inside" to the "outside".

We have chosen our unit of length by setting $t = 1$. The units of time are arbitrary. In Figs. 5-9 negative velocity indicates motion directed "inward", i.e., from $\rho = 1$ to $\rho = 4$. An example will clarify these points: a shell 10 μm thick with perturbations of $\lambda = 30$ μm on its outer and inner surfaces is stationary at $\tau = 0$. Assume that it moves according to Fig. 6a, and that time is measured in nanoseconds. Then at $\tau =$ 1 ns the shell jumps inward with speed 20 μm/ns, and immediately afterwards accelerates inward with $|g| = 20$ μm/ns^2 until $\tau = 4$ ns, at which time it

is moving inwards at 80 μm/ns. We will call this maximum speed its "implosion velocity". At τ = 4 ns the shell decelerates with $|g|$ = 30 $\mu m/ns^2$ until τ = 5 by which time its speed is reduced to 50 μm/ns. A shock at τ = 5 ns brings the shell to rest; it has covered a total distance of 215 μm.

The results of our calculations corresponding to the velocity histories of Fig. 5a, 6a, 7a, 8a, and 9a are shown in Fig. 5b, 6b, 7b, 8b, and 9b respectively. In all these calculations the density profile is given in Fig. 2c, λ = 3t, and $\eta_1(o) = \eta_4(o) = \eta(o)$, with other η's and $\dot{\eta}$'s equal to zero initially. In these figures we show $\eta_1(\tau)/\eta(o)$ and $\eta_4(\tau)/\eta(o)$, the "outside" and "inside" perturbations, as functions of time τ.

We do not show the internal perturbations, $\eta_2(\tau)$ and $\eta_3(\tau)$, which start from zero and by $\tau \simeq 5$ are of the same order as the average of η_1 and η_4.

For a number of cases we carried out a parallel calculation in which we used the classical equations, Eqs. (1) and (2), to evolve the perturbations at each interface. This reproduced the outside perturbations to within an order of magnitude, but the inside perturbations were off by more than an order of magnitude, and sometimes by two orders of magnitude by the time $\tau \simeq 5$. Of course, according to the classical expression Eq. (1), the inner surface, having Attwood number -1, is stable during the inward acceleration phase and oscillates, while according to Eq. (4) the inner surface is coupled to the outer unstable surface where perturbations grow and drive perturbations in the rest of the fluid.

The coupling between interfaces is most clear at $\tau = 5$, by which time the outer perturbation grows very large and "takes over": the phase reversal of this outer perturbation immediately after the last shock (which brings the system to rest) is expected on classical grounds, since the shock, directed from inside out, proceeds from a high ($\rho = 1$) to low ($\rho = 0$) density at the outer surface. What is difficult to explain is the phase reversal at the inner surface where the shock proceeds from low density ($\rho = 0$) to high density ($\rho = 4$). This phase reversal can be understood if we remember that by this time the large outer perturbation controls the rest of the perturbations; in other words, the inner perturbations reverse their phase because the outer perturbations have.

Figures 5-9 show that by $\tau \simeq 5$ perturbations have increased almost by a factor of about 10^3. As mentioned earlier, shorter wavelength perturbations grew even more, particularly on the outer surface, and our choice of $\lambda = 3t$ was partly motivated by reasonable estimates of surface finish and how much growth can be tolerated because our calculation breaks down when non-linear effects come into play. Going back to our example of a shell 10 μm thick, it is reasonable to assume an initial surface finish of $\eta(o) \gtrsim 100$ Å. Growing thousand-fold this amplitude reaches $\eta \gtrsim 10$ μm and is barely within the linear regime since $\lambda = 30$ μm. Clearly, choosing a shorter wavelength which grows faster would have taken us well beyond the linear regime and the validity of our theory unless, of course, we assumed a much smaller initial amplitude.

In Figs. 5-9 three out of the four inputs are kept fixed (same density profile, same wavelength, and same initial conditions on the η_i). Only the fourth input, viz. the velocity history, is varied in Figs. 5-9. The

growth of the perturbations clearly depends on the velocity history of the shell, as these figures illustrate.

Finally, we show an example of how a perfectly smooth outer surface develops perturbations as large as the case of an initially rough outer surface. In Fig. 10 we show how perturbations evolve from the initial values $\eta_{outside}(o) = 0$ and $\eta_{inside} = \eta(o)$, i.e., all surfaces start perfectly smooth except for the inside surface. The velocity history is that of Fig. 6a. Comparing Fig. 6b and Fig. 10b we see that an initially smooth outer surface does not necessarily suppress the growth of perturbations at later times - a perturbation at only one interface can act as seed for perturbations throughout the fluid.

V. COMMENTS AND CONCLUSIONS

(i) We ran a number of tests to check the code: first, at short wavelengths the interfaces decouple because the off-diagonal matrix elements of M in Eq. (3) go to zero like $1/\sinh(kt_i)$, and the results agree with the classical expressions. Second, for N = 3 the code gives the same results as in Eqs. (12) and (13) for the case $\rho_1 = \rho_3 = 0$. Third, the four eigenvalues calculated by the code for the density profile shown in Fig. 2c and for $\lambda = 3t$ are $\gamma/\sqrt{g} = 1.447, 0.821, 0.553$, and $1.447i$; these numbers agree very closely with the expressions given in the previous Section (see Eq. (18) and the discussion preceeding it). Finally, Figs. 5 and 9 show that if the velocity histories are sufficiently similar, then the perturbations evolve similarly. In fact, Fig. 9 was run just to check if a series of small shocks can imitate a constant acceleration: the velocity history shown in Fig. 5(a) is a combination of shocks and accelerations, hence the perturbations were

evolved using both Eq. (4) and (6), while the velocity history of Fig. 9(a) consists entirely of shocks, and is similar to Fig. 5(a) except that the constant acceleration between $\tau = 2$ and $\tau = 4$ is replaced by a number of small shocks. Hence only Eq. (6) is used to evolve the perturbations, and the result, shown in Fig. 9(b), is quite similar to Fig. 5(b).

Clearly, an acceleration history that varies continuously with time can also be treated in this fashion by breaking it down into a series of small shocks and constant accelerations and using the appropriate equation in each time step.

(ii) Before applying our techniques to an actual system, one must of course check if the assumptions of linearity, incompressibility, no heat transfer, no viscosity and no surface tension are satisfied. The examples treated in the previous section were inspired from ICF implosions. A number of complex processes are involved, and no doubt our techniques will never replace full 2D hydro calculations of the Rayleigh-Taylor instability as reported in the literature.[8] Instead, our code can serve as a post-processor code in which density profiles and velocity histories are read from a 1D hydro code. That information, combined with reasonable estimates of initial surface finish, is used to evolve perturbation amplitudes in time. Such post-processing will require much less computing time and effort though the results, of course, will not be as reliable as the full 2D hydro results because of all the assumptions that go into the derivation of the evolution equations, Eqs. (4) and (6).

For ICF implosions, while surface tension and viscosity are practically absent, realistic initial amplitudes can quickly evolve into the non-linear regime where our equations break down. Furthermore, we cannot justify the

assumption of no heat transfer in ICF capsules since the shells are driven by ablation. A number of calculations[9,8] indicate that ablation reduces the growth rates for Rayleigh-Taylor instabilities, in which case we would be overestimating the growth at the outer surface. This would have important consequences since, as discussed in the previous Section, the inner perturbations are driven largely by the growth of the outer perturbations. If a mechanism stabilizes the outer surface, then we have reason to expect that the inner perturbations also will not grow very large. We must point out, however, that other 2D hydro calculations[10] do not show a reduction in the growth rate and that there is no clear experimental evidence for such stabilization.

While our calculations do not take this possible effect into account, they highlight its importance. Indeed, when we artificially put a limit of 50 on the outer perturbation, the inner perturbation also grew less.

(iii) Finally, we discuss the assumption of incompressibility. For the case of the Rayleigh-Taylor instability it is not yet clear whether the effect of compressibility is to cause an increase or decrease in the growth rate (see Ref. 11). In the case of the Richtmyer-Meshkov instability the effects of compressibility would be even more important, since real fluids invariably get compressed upon the passage of a shock.

One approximate remedy is to change the density profile also as a function of time. Of course, this involves more calculations since the eigenvalues and eigenfunctions have to be calculated all over again with each new density profile, but in principle it can be done within our formalism. Another effect that has to be taken into account is the finite shock transit time: clearly a real shock starting at the outer surface takes a finite

period of time to break through the inner surface, while in our formalism the system as a whole acquires an instantaneous velocity jump.

It is difficult to estimate how much our theory suffers because of the underlying assumption of imcompressibility. On one hand we probably overestimate the effect of interface coupling: an interface that has not yet been shocked should not affect the perturbation at interfaces that have already been shocked; but in our formalism all interfaces feel the shock simultaneously and hence the eigenfunctions $W(i,\ell)$ are established instantaneously. On the other hand, we probably underestimate the effect of interface coupling because our eigenfunctions decay exponentially at long distances, while in a compressible theory we expect them to decay as some power law. It could be that these two opposing tendencies cancel each other out to some extent, but at present we have no means of estimating the net effect.

Given the assumptions that go into the derivation of the classical expression

$$\frac{d\eta}{d\tau} = \eta \Delta v k \frac{\rho_2 - \rho_1}{\rho_2 + \rho_1} \tag{19}$$

it is indeed surprizing that experiments and numerical calculations with compressible fluids gave results consistent with it: Richtmyer's numerical calculations[3] were consistent with Eq. (19) provided he used the post-shock, i.e., compressed amplitude and the post-shock densities in this equation. He considered a shock proceeding from a light to a heavy fluid. Subsequent numerical calculations by Meyer and Blewett[12] agreed with Richtmyer's results and, for the case of a shock proceeding from a heavy to a light fluid, they suggested using the average of pre-shock and post-shock amplitudes in Eq.

(19) (of course, for incompressible fluids these prescriptions give the same answer since pre-shock and post-shock densities and perturbation amplitudes are the same). Experiments by Meshkov[4] were also consistent, within a factor of ~ 2, with Eq. (19), and confirmed the fact that perturbations grow linearly with time whether the shock proceeds from light to heavy or from heavy to light fluids.

Thus there is some evidence that the classical expression, in which a shock is treated as an impulsive acceleration, does a reasonably good job for the case N = 2. Whether our extension to arbitrary N is also reasonable remains to be seen by new calculations and experiments.

ACKNOWLEDGEMENTS

I am greatful to Gene Burke and Viviane Rupert for bringing the problem of shock initiated instabilities to my attention. John Nuckolls and John Lindl have made valuable suggestions.

REFERENCES

1. Lord Rayleigh, Scientific Papers (Dover, New York, 1900) Vol. 2.
2. G. I. Taylor, Proc. Ray. Soc. London Ser. A 201, 192 (1950).
3. R. D. Richtmyer, Comm. Pure and Appl. Math., Vol. 13, 297 (1960).
4. E. E. Meshkov, Izv. Akad. Nauk SSSR, Mekh. Zhidk. Gaz. No. 5, 151 (1969).
5. V. A. Andronov et al., Zh. Eksp. Teor. Fiz. 71, 806 (1976) [Sov. Phys. JETP, Vol. 44, 424 (1976)].
6. K. O. Mikaelian, Phys. Rev. Lett. 48, 1365 (1982); Phys. Rev. A 26, 2140 (1982).
7. K. O. Mikaelian, Phys. Rev. A 28, 1637 (1983).
8. R. L. McCrory, L. Montierth, R. L. Morse, and C. P. Verdon, Phys. Rev. Lett. 46, 336 (1981); M. H. Emery, J. H. Gardner and J. P. Boris ibid 48, 677 (1982); R. G. Evans, A. J. Bennett and G. J. Pert, ibid 49, 1639 (1982).
9. S. E. Bodner, Phys. Rev. Lett. 33, 761 (1974).
10. J. D. Lindl and W. C. Mead, Phys. Rev. Lett. 34, 1273 (1975).
11. I. B. Bernstein and D. L. Book, Phys. Fluids 26, 453 (1983).
12. K. A. Meyer and P. J. Blewett, Phys. Fluids 15, 753 (1972).

FIGURE CAPTIONS

Fig. 1 N fluid layers of density $\rho_1, \ldots, \rho_N$ and thickness $t_1, \ldots, t_N$ which are stacked in the direction of acceleration $\hat{g} = \hat{y}$, where g = constant for Rayleigh-Taylor and $g = \Delta v\, \delta(\tau - \tau_s)$ for Richtmyer-Meshkov instabilities. Unperturbed densities are uniform in the x and z directions, and vary only in the y direction. The amplitude of sinusoidal perturbations at each interface i is denoted by η_i. The wavelength of the perturbations is λ.

Fig. 2 (a) The density profile for the classical case N = 2 with one interface. (b) The density profile for N = 3 and for the special case $\rho_1 = \rho_3 = 0$, $\rho_2 = \rho$ and $t_1 = t_3 = \infty$, $t_2 = t$.
(c) The density profile for N = 5 with densities (0, 1, 2, 4, 0) and thicknesses (∞, t/3, t/3, t/3, ∞). The amplitudes $\eta_{outside}$ and η_{inside} refer to perturbations at the first and last interfaces, respectively.

Fig. 3 Possible evolution patterns of the amplitude for the classical case N = 2. η is the amplitude of perturbations at the interface between ρ_1 and ρ_2 (see Fig. 2a). The system is assumed to be coasting until time τ_s, at which time a shock induces a jump velocity Δv. Only diagrams (a) to (i) are allowed if the shock proceeds from a high to a low density. In the opposite case where the shock proceeds from a low to a high density, only diagrams (i) to (o) are allowed. It is possible to "freeze out" an amplitude as indicated in diagrams (c), (g) and (n).

Fig. 4 The simplest case for N = 3: a fluid layer of density ρ and thickness t having two free boundaries (see Fig. 2b). Initially one surface is perturbed while the other is perfectly smooth. Perturbations at each surface evolve according to Eqs. (14) and (15).

Fig. 5 (a) A velocity history describing the motion of a shell whose density profile is shown in Fig. 2(c). Negative velocities are directed from outside to inside. The shell thickness t is chosen as scale for length or distance. Units of time τ are arbitrary. $D = \int_0^6 v d\tau$. In this case the shell covers a distance D of 12.0 times its thickness. (b) Evolution of perturbations at the outer and inner surfaces of the shell, assuming the velocity history of diagram (a). Initially the outer and inner surfaces have perturbations of amplitudes $\eta(o)$ and wavelength $\lambda = 3t$.

Fig. 6 Same as Fig. 5 for a different velocity history. The system covers a distance of 21.5 times the shell thickness.

Fig. 7 Same as Fig. 5 for a different velocity history. The distance covered is 20.0 times the shell thickness.

Fig. 8 Same as Fig. 5 for a different velocity history consisting entirely of shocks. The distance covered is 19.0 times the shell thickness.

Fig. 9 Same as Fig. 5 for a velocity history similar to Fig. 5a in which the constant acceleration between $\tau = 2$ and $\tau = 4$ is replaced by a series of five small shocks. Compare with Fig. 5.

Fig. 10 Same as Fig. 6 but with different initial conditions: only the inner surface has initial perturbations; the outer surface starts perfectly smooth. Compare with Fig. 6.

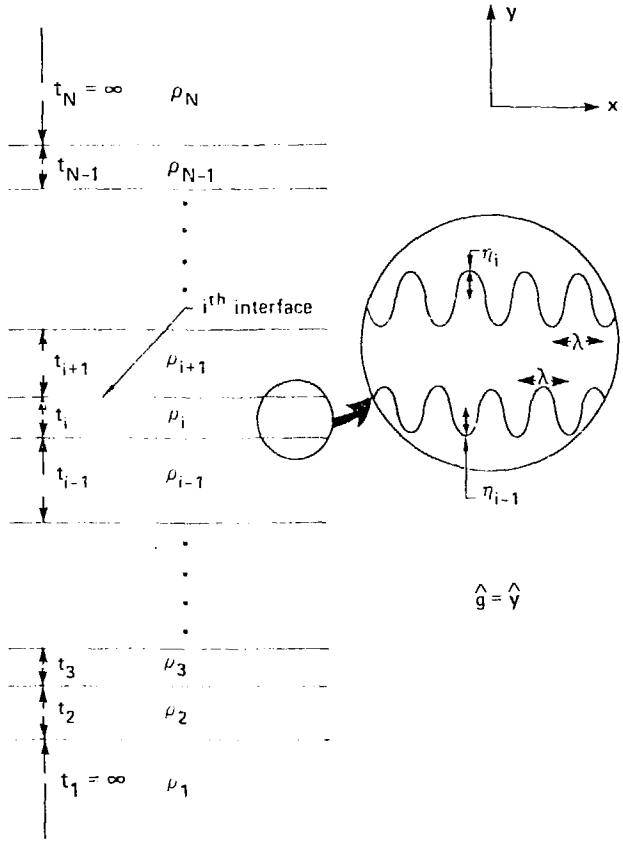
y
x
$t_N = \infty$
ρ_N
t_{N-1}
ρ_{N-1}
i^{th} interface
t_{i+1}
ρ_{i+1}
t_i
ρ_i
t_{i-1}
ρ_{i-1}
t_3
ρ_3
t_2
ρ_2
$t_1 = \infty$
ρ_1
η_i
λ
λ
η_{i-1}
$\hat{g} = \hat{y}$

Fig. 1

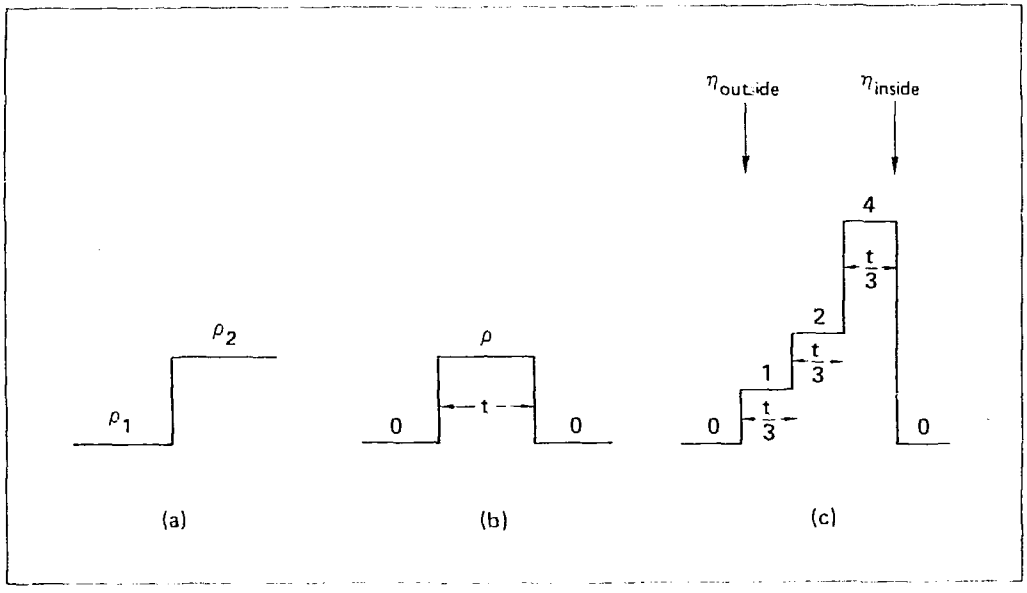
$\eta_{outside}$
η_{inside}
ρ_2
ρ_1
ρ
0
t
0
4
2
1
0
$\frac{t}{3}$
$\frac{t}{3}$
$\frac{t}{3}$
0
(a)
(b)
(c)

Fig. 2

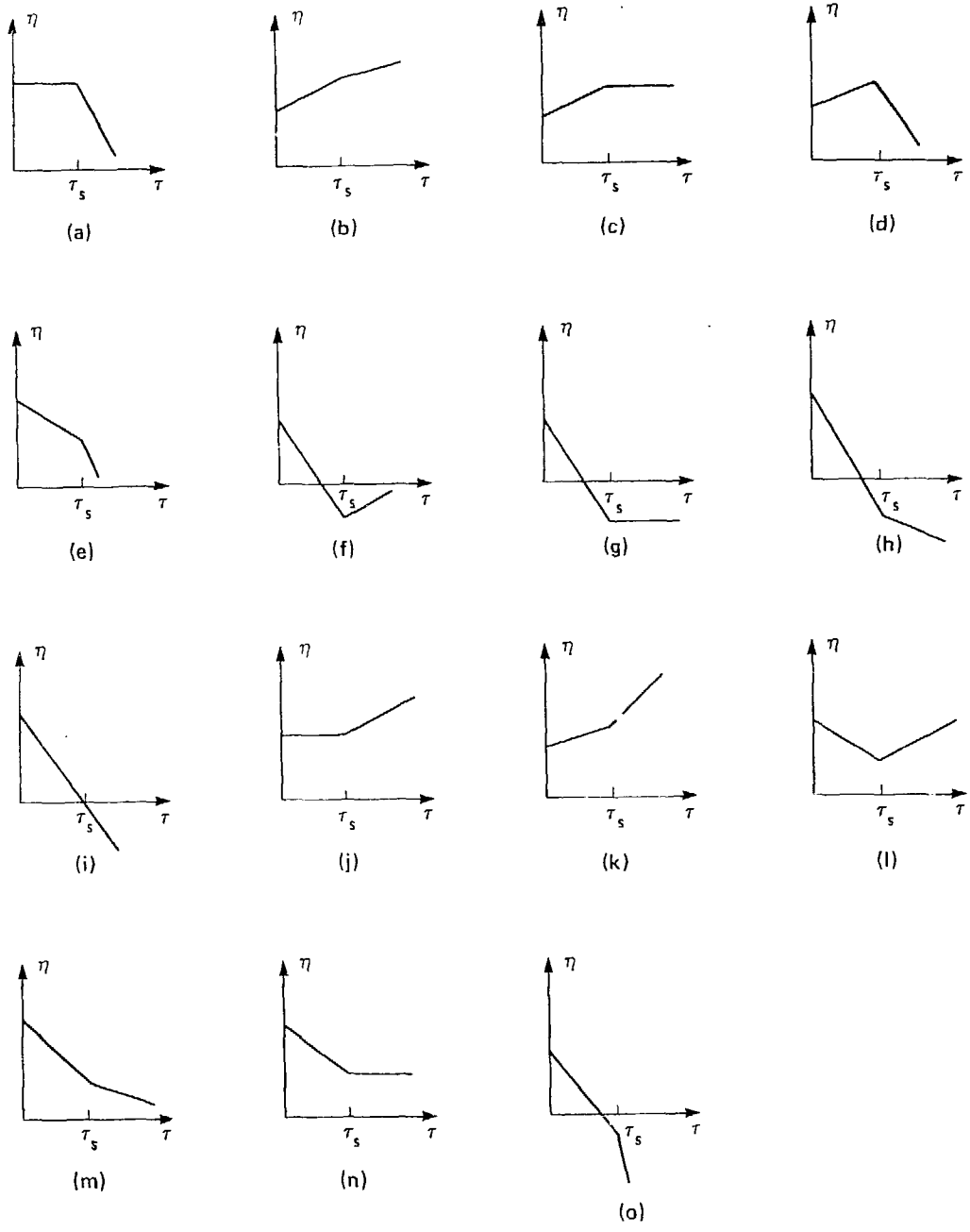

Fig. 3

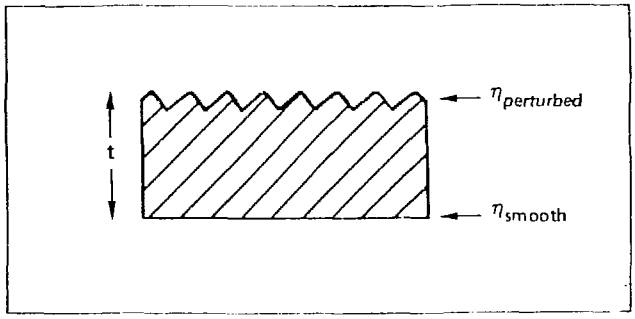

Fig. 4

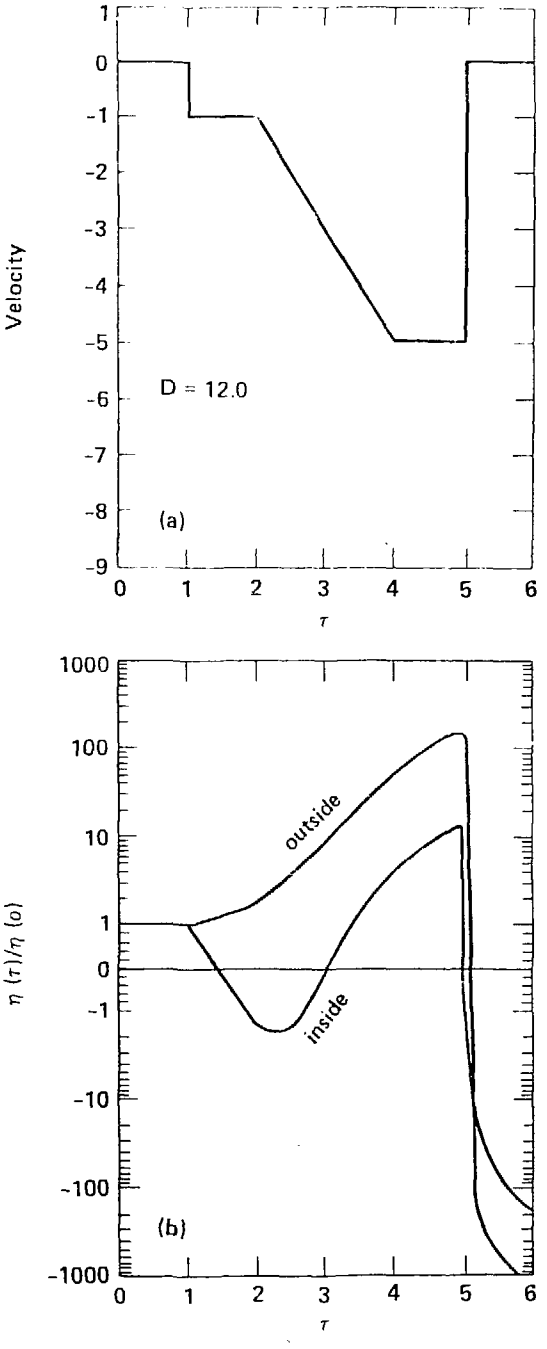

Fig. 5

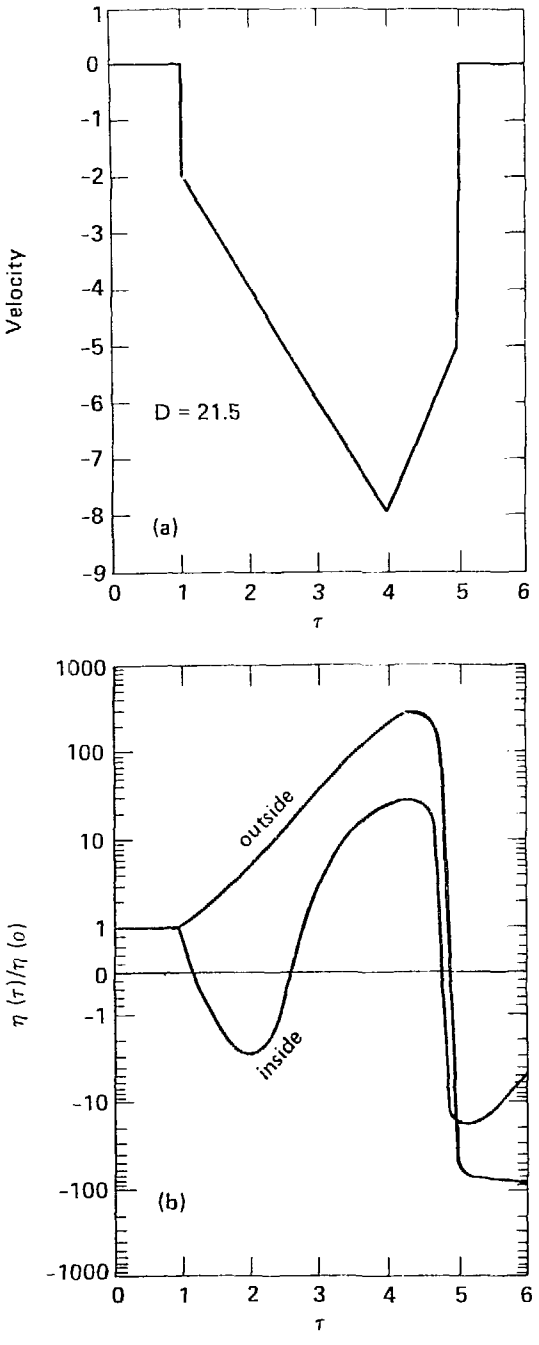
Velocity
1
0
-1
-2
-3
-4
-5
-6
-7
-8
-9
D = 21.5
(a)
0
1
2
3
4
5
6
τ
1000
100
10
1
0
-1
-10
-100
-1000
η (τ)/η (o)
outside
inside
(b)
0
1
2
3
4
5
6
τ

Fig. 6

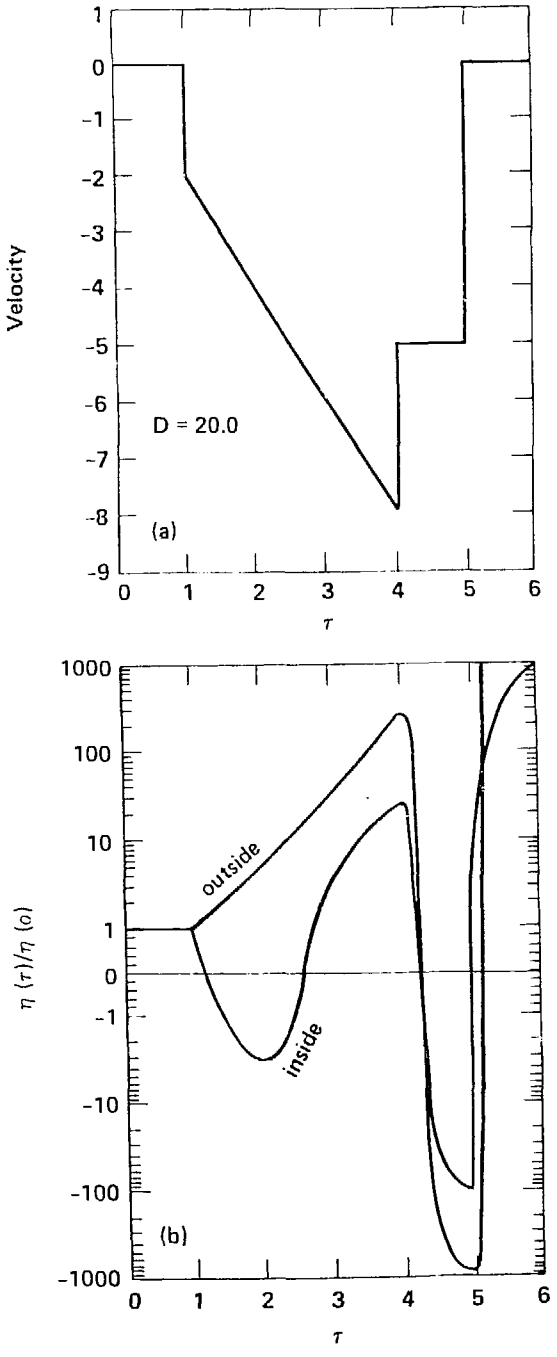
Velocity
1
0
-1
-2
-3
-4
-5
-6
-7
-8
-9
D = 20.0
(a)
0 1 2 3 4 5 6
τ
1000
100
10
1
0
-1
-10
-100
-1000
outside
inside
(b)
η (τ)/η (o)
0 1 2 3 4 5 6
τ

Fig. 7

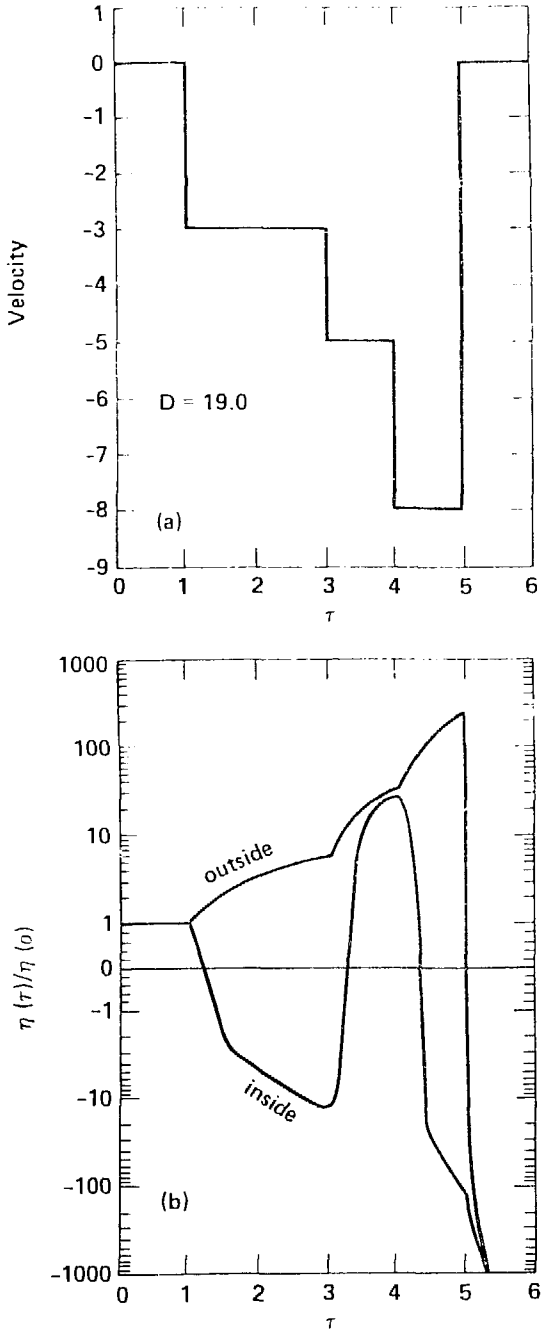

Fig. 8

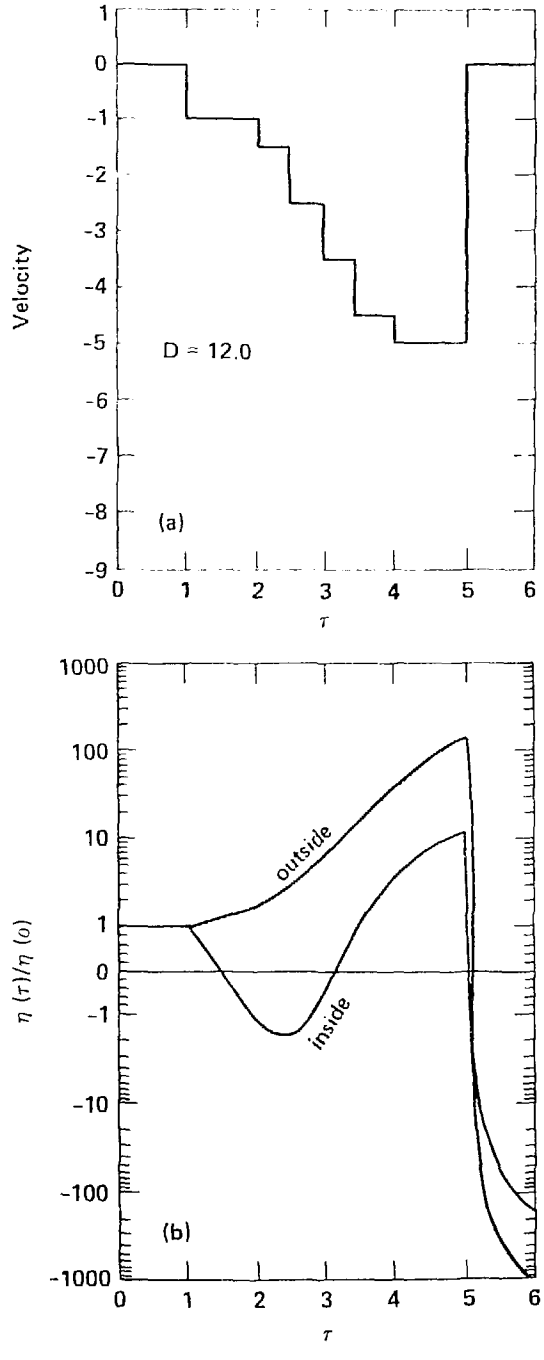

Fig. 9

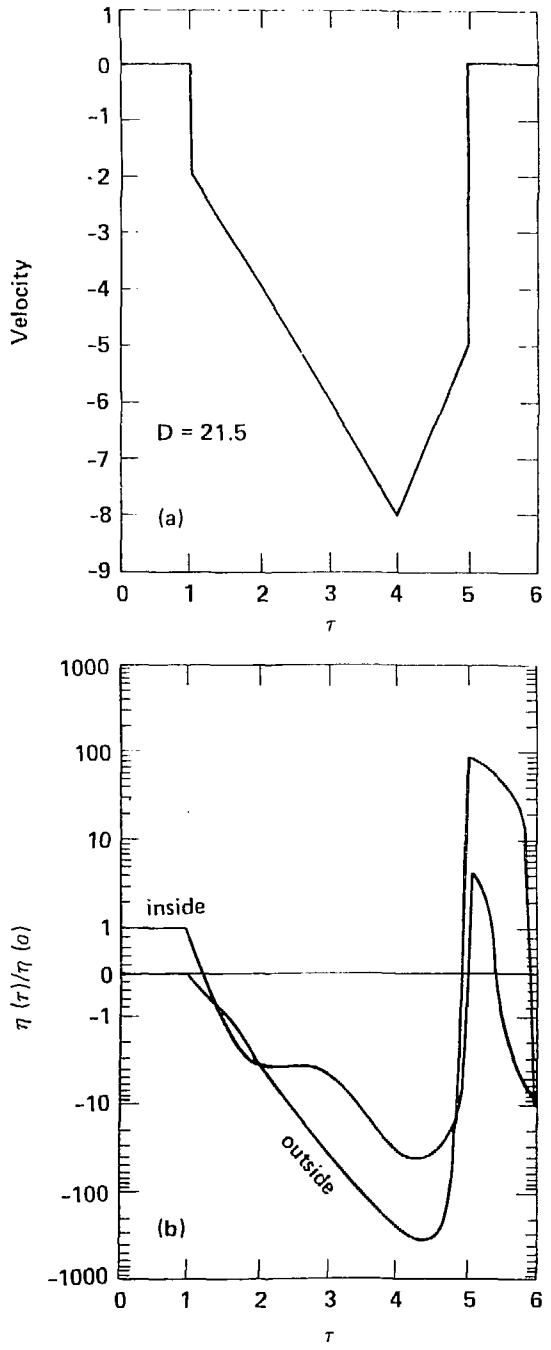

Fig. 10